Theor Chem Acc (2011) 128:727–734
DOI 10.1007/s00214-010-0787-6

REGULAR ARTICLE

On the anomaly of the quasiclassical product distributions of the OH + CO → H + CO_2 reaction

E. Garcia · A. Saracibar · A. Laganà

Received: 6 May 2010 / Accepted: 19 July 2010 / Published online: 12 August 2010

Abstract A grid empowered molecular simulator (GEMS) embodying in a single workflow the ab initio treatment of elementary chemical processes has been extended to four atom reactions. GEMS has been used to carry out a massive quasiclassical investigation for the OH + CO → H + CO_2 reaction on the most recently proposed potential energy surface. The type of potential energy surface used and the possibility of running the simulations on the grid have allowed us to keep the error of the order of a few percent at all values of the collision energy and to estimate accurately the dependence of the reaction cross section on the collision energy. The accuracy of the calculations has allowed to unequivocally single out the fact that the calculated center-of-mass angular distribution is clearly isotropic and radically differs from the asymmetric forward–backward structure obtained from the experiment. However, when the laboratory frame analogues are compared, the difference almost vanishes.

Keywords Reactive scattering · OH + CO reaction · Quasiclassical trajectories · Product distributions · Molecular simulator · Chemistry on grid

Published as part of the special issue celebrating theoretical and computational chemistry in Spain.

E. Garcia (✉) · A. Saracibar
Departamento de Quimica Fisica, Universidad del Pais Vasco, Vitoria 01006, Spain
e-mail: e.garcia@ehu.es

A. Laganà
Dipartimento di Chimica, Università di Perugia, Perugia 06123, Italy
e-mail: lag@dyn.unipg.it

1 Introduction

The hydroxyl radical-carbon monoxide, OH + CO → H + CO_2, reaction is important for combustion and atmospheric chemistry modeling. It is, in fact, the main source of CO_2 and energy release in hydrocarbon combustion [1, 2] as well as the key reaction for the control of the concentration of the OH radical in the lower atmosphere [3, 4].

Thermal rate coefficients of the title reaction were measured in the temperature interval 80–2,800 K [5–11]. These values show a strong non-Arrhenius behavior and were given an analytical formulation using an RRKM scheme in Refs. [12–16]. Experimental estimates of the absolute cross section of the OH + CO reaction were provided by Wolfrum and collaborators [17, 18], while those of the differential cross section were provided by Casavecchia and collaborators in their crossed molecular beam (CMB) studies [19–21]. In particular, they measured the product intensity $I_{\rm lab}(\Theta', w')$ at several values of the laboratory (lab) angle Θ' (product variables are primed). Then, they factorized $I_{\rm lab}(\Theta', w')$ for the allowed range of values of the recoil velocity w' in a tentative center-of-mass (cm) product angular distribution (PAD), $T(\theta')$, and a tentative cm product translational energy distribution (PTD), $P(E'_{\rm tr})$ (with θ' and $E'_{\rm tr}$ being the cm scattering angle and translational energy, respectively). In this way, Casavecchia and collaborators were able to work out the PAD and the PTD at the two collision energy values ($E_{\rm tr}$ = 36 and 59 kJ mol^{-1}) of the experiment. The resulting PAD exhibits in both cases a forward-backward structure with a clear preference for the forward direction. This was interpreted as a fingerprint of a reactive mechanism proceeding through an intermediate complex. At the same time, the resulting PTD shows (again in both cases) that a large fraction of energy goes in product translation. This was

interpreted as fingerprint of the strong repulsive interaction taking place between CO_2 and H in the exit channel.

Previous theoretical work focused on the analysis of the dissociation of the intermediate complexes using both RRKM [22–25] and dynamical [26–48] treatments. A first computational challenge of the theoretical study is the accurate ab initio determination of the quite structured nature of the ground-state potential energy surface (PES). The OH + CO PES, in fact, exhibits different stationary points and multiple reaction paths. This has made it difficult not only to carry out a comprehensive ab initio determination of the interaction but also its full-dimensional fit to a suitable functional representation. As a matter of fact, only fairly recently, following the work of Schatz et al. [49], two full-dimensional PESs (LTSH [37] and YMS [50]) were fitted to the ab initio electronic energies. For this purpose, a many-body expansion (MBE) functional [51] was used, and various gaussians were added to enforce the reproduction of some local structures of the ab initio data. Yet, trajectories calculated on them showed to be affected by some numerical instabilities and to lead to a poor conservation of total energy [37, 47]. These difficulties were more recently circumvented by adopting a new PES [41]. The proposed (Leiden) PES is full-dimensional representation of the interaction based on the Shepard interpolation of a set of high-level ab initio estimates (linear combination of DFT and CCSD(T) energies) of the potential energy values together with their first and second derivatives generated iteratively using the Collins' GROW program [52]. This makes the computation of the single molecular geometry potential energy value much more expensive than for the LSTH and YMS PESs.

For this reason, the only way of compacting the whole ab initio calculation (from the determination of the PES to the dynamical computation and estimate of the measured quantities) is via a grid-based workflow as it has been already made for atom-diatom systems [53–56]. Unfortunately, a rigorous quantum study of the dynamics of this four atom reaction is still out of reach [39, 40]. Therefore, in order to work out a theoretical estimate of the quantities measured in a CMB experiment [19–21], we had to extend the mentioned workflow to the VENUS package [57], a computational dynamical engine integrating the quasi-classical trajectories (QCT) for polyatomic systems. The study was then completed by carrying out a comparison also with the dynamical properties calculated on the YMS and LTSH PESs.

Accordingly, the paper is articulated as follows: In Sect. 2, an analysis of the Leiden PES is carried out and the details of the calculations are described; in Sects. 3 and 4, the values of the reactive cross sections and cm product distributions calculated on the various PESs are compared among them and with the experiment; finally, in Sect. 5, the rationalization of the experimental laboratory angular distribution using the QCT outcomes is performed.

2 The calculations

As already mentioned, the evaluation of a single molecular geometry potential energy value for the $OH + CO \rightarrow H + CO_2$ elementary reaction is, by itself, a highly computationally demanding task. When one needs to calculate it for millions of trajectories each exploring in time steps of 0.01 fs the articulated structure of a realistic PES, the problem may become a real computational challenge.

To illustrate the complexity of the Leiden PES, a schematic representation of its stationary points is given in Fig. 1. As apparent from the figure, the main characteristics of the PES are the two intermediate wells corresponding to the trans-HOCO and the cis-HOCO complexes (with the former being slightly deeper). These wells are divided by an interposed relatively small barrier. Each well is also separated from reactants by a small barrier (with the one for the cis well being higher). The long-range interaction between the reactant molecules is however attractive, and related minimum energy paths show a van der Waals well. The production of $H + CO_2$ goes through a relatively high barrier for the cis-HOCO complex and an even higher barrier for the trans-HOCO complex. Therefore, following the minimum energy path, the trans-HOCO complex has to surmount two high barriers (trans-HOCO-HCO_2 and trans-H-OCO) before landing into the products valley. The smaller one (but higher than that connecting the cis-HOCO complex to products) leads to a new well with C_{2v} symmetry, which is connected to the products via a relatively small barrier. The second barrier is instead significantly higher and leads directly into the product valley. This barrier is substantially higher than those of the YMS and

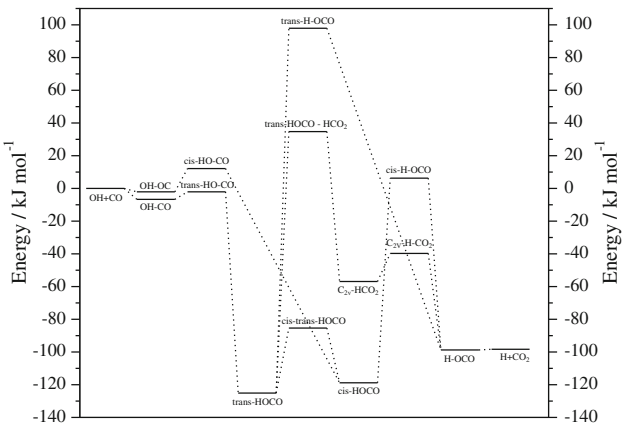

Fig. 1 A schematic representation of the stationary points of the Leiden PES for the $OH + CO \rightarrow H + CO_2$ reaction

LTSH PESs whose height is similar to the cis-H-OCO one. Also, the trans-HOCO-HCO_2 barrier of the Leiden PES is 1.7 kJ mol^{-1} higher than those of the YMS and LTSH PESs. The product channel too is attractive and forms a van der Waals complex. It is worth mentioning here that the internal energy of the reactants in the ground vibrotational states is 35.1 kJ mol^{-1}. This energy is higher than the two barriers that connect the HOCO complexes to the product channels (namely trans-HOCO-HCO_2 (34.7 kJ mol^{-1}) and cis-H-OCO (6.3 kJ mol^{-1})) while it is 62.8 kJ mol^{-1} lower than the one necessary to surmount the trans-H-OCO barrier (97.9 kJ mol^{-1}).

The associated computational burden has been mastered by distributing the calculations among high-performance and high-throughput concurrent platforms [58–60] using a properly extended version of GEMS [53–56]. GEMS, in its most recent version, allows the running of large batches of four atom trajectories using a parameter sweeping scheme. In this scheme, the batches of trajectories are run concurrently by distributing them over the several thousands of CPUs conferred to the segment of the EGEE grid available to the virtual organization COMPCHEM [61]. It is worth pointing out here that this is the first time that GEMS is extended to deal with four atom reactions. The main novelty consists in the fact that GEMS now embodies in a single workflow three new features: the treatment of a four atom PES, a QCT treatment of diatom–diatom elementary chemical process and the evaluation of the laboratory-measured intensity $I_{\mathrm{lab}}(\Theta', w')$ out of the computed $I_{\mathrm{cm}}(\theta', u')$ (or $T(\theta')$ and $P(u')$).

To this end, two large batches of jobs targeted to the evaluation of both the PTD and PAD associated with the conditions of the beam experiment [19–21] (OH and CO molecules set at their ground vibrotational states $v_{\mathrm{OH}} = j_{\mathrm{OH}} = 0$ and $v_{\mathrm{CO}} = j_{\mathrm{CO}} = 0$ and translational energies set at $E_{\mathrm{tr}} = 36$ and $E_{\mathrm{tr}} = 59$ kJ mol^{-1}) were launched. The PTD and PAD calculations have been repeated also for the first excited vibrational state of OH $v_{\mathrm{OH}} = 1$ and $j_{\mathrm{OH}} = 0$ though only at $E_{\mathrm{tr}} = 36$ kJ mol^{-1}. In addition, a massive calculation running several batches of jobs targeted to the evaluation of the reaction cross section for a fine grid of collision energy values falling in the interval ranging from 1 to 77 kJ mol^{-1} was also performed.

In QCT calculations, the integration step was set at 0.01 fs in order to guarantee a good conservation of the total energy. It is worth noting here that the QCT calculations using the Leiden PES do not show any instabilities with respect to the total energy conservation. In fact, using the time step of 0.01 fs, one typically makes an error lower than of 10^{-5} and 10^{-4} kJ mol^{-1} in the conservation of total energy for non-reactive and reactive trajectories, respectively. This is not the case of the QCT calculations performed on the YMS and LTSH PESs for which more than 30 and 70% of the non-reactive and reactive trajectories, respectively, have a energy conservation poorer than 0.16 kJ mol^{-1}.

For all trajectories, initial and final distances were set at 8.0 Å, a distance large enough to consider negligible the interaction between the fragments of the related channels. The value of the maximum impact parameter was varied (according to the collision energy) from 2.2 Å (at high energy) to 3.0 Å (at low energy). All remaining parameters (vibrational phases and spatial orientation of molecules) were selected randomly. Calculated values of the cross sections were scaled using the statistical factor of 1/2 (to account for the double degeneracy of the OH($^2\Pi$) electronic state). The calculations do not include any zero point energy (ZPE) correction or any other quantum effect. However, at the energies of the experiment considered here, quantum effects are not expected to play a major role. In any case, the introduction of the ZPE correction would no improve the agreement of calculations with the experiment because its effect would be to increase the threshold and further reduce the theoretical estimate of the product translational energy that is already too low.

The number of trajectories integrated to evaluate the cross section ranges from 100,000 at high collision energy to more than 4 million at the lowest collision energy so as to keep the relative error of the calculated reaction cross section smaller than 5%. Many more trajectories (9 and 11 million at the collision energy values of 59 and 36 kJ mol^{-1}, respectively, with more than 40,000 trajectories being reactive in each case) were integrated when calculating the PTDs and PADs to be compared with CMB results.

3 The reaction cross section

QCT values of the cross sections calculated on the Leiden PES for the collision energy interval ranging from 1 to 77 kJ mol^{-1} are plotted in Fig. 2 (solid circles connected by dashed lines) as a function of the collision energy (this quantity is also called excitation function). For comparative purposes, the figure shows also the experimental cross section data reported in Refs. [17, 18] as well as the QCT results reported in Refs. [37, 41, 47]. As mentioned in Ref. [47], the factor 1/2 has been applied also to the results of Refs. [41] and [37] in order to make the comparison homogeneous.

As apparent from the figure, the excitation function calculated on the Leiden PES shows a positive trend with the collision energy for the whole energy interval considered in agreement with the results previously reported for a narrower interval [41]. The cross section, though, increases mildly and almost linearly in contrast with the steeper increase found for the YMS results. Cross sections

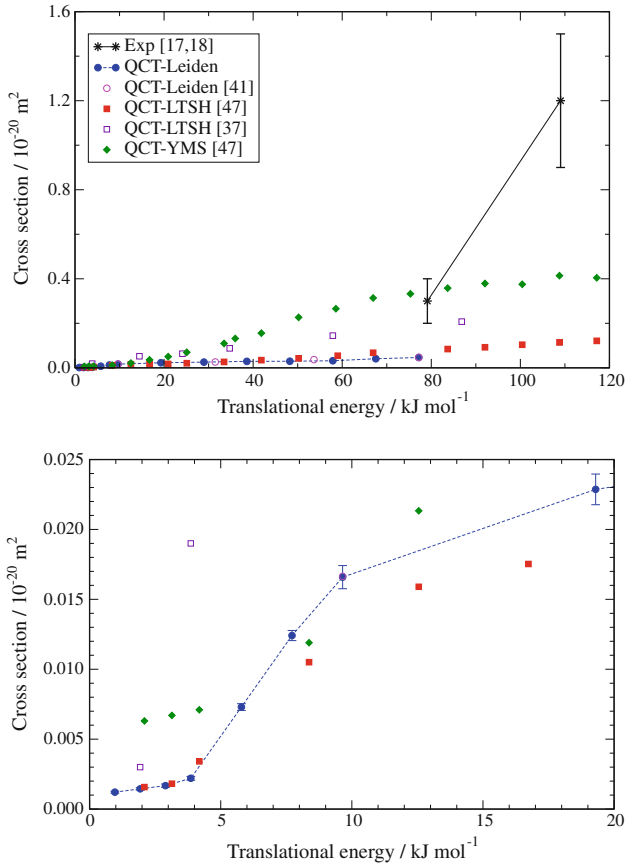

Fig. 2 (*Upper panel*) QCT cross sections calculated on the Leiden PES plotted as *solid circles* connected by dashed lines against translation energy. Experimental values of Refs. [17, 18] are given as stars connected by *solid line*. QCT results of previous calculations or performed on other PESs (*open circles*, *open squares*, *solid squares*, *solid diamonds*) are also shown. (*Lower panel*) a zoom on the low translation energy region for the same results

calculated on the LTSH PES agree fairly well with those calculated on the Leiden PES for about the whole range of collision energy values (at large collision energy, the LTSH results are slightly higher). This agreement contrasts with the findings of Ref. [41] where the comparison is made with the results of Ref. [37]. However, it is important point out here that the cross sections obtained in Ref. [37] on the LTSH PES differ non-negligibly from those of Ref. [47] calculated on the same PES due to the different filter adopted for discarding poorly energy conserving trajectories. This suggests that the different energy conserving filtering criterion (rather than the one invoking in Ref. [41] the higher barrier separating the trans-HOCO minimum from the product valley (97.9 kJ mol^{-1} in the Leiden PES, 9.6 kJ mol^{-1} in the LTSH one) should be preferred in order to rationalize the lower values of the Leiden cross sections with respect to the LTSH ones.

A comparison of the calculated cross section values with the experimental ones is also shown in Fig. 2. This comparison is not fully quantitative because calculations have been carried out with both reactants in their ground vibrotational states while in the experiment significantly excited (up to $j_{OH} = 20$) rotational levels of OH are involved [47]. This may offer a rationale for why computed and measured values increasingly differ as energy increases. However, it has to be said also that experimental estimates of the cross section have been questioned in the past and a revision of the related calibration method has been suggested [41, 62].

As apparent from the lower panel of Fig. 2 that zooms on the very low collision energy region (not explored in Ref. [41]), the excitation function calculated by us on the Leiden PES exhibits a clear switch in slope in the translational energy interval ranging from 4 to 10 kJ mol^{-1}. A similar trend is also exhibited by the LTSH results. A further lowering of the collision energy does not cancel completely the reactivity calculated on all the mentioned PESs building a clear uncertainty on the evaluation of the threshold. This is due to the fact that at low collision energy the main contribution to reaction is given by internal energy.

In order to gain more insight into the mechanisms fueling reaction, we found it useful to perform an analysis of the dihedral angle of the products (i.e. the angle that by the CO_2 plane and the plane containing the scattered H atom and the additional (produced by the reaction) CO bond) form. This dihedral angle carries information on the geometry of the complex at the moment of breaking the OH bond to react. Accordingly, if the breaking complex is the cis-HOCO one, the H atom is expected to be scattered mainly with a low (ideally 0°) dihedral angle. On the contrary, the breaking of the trans-HOCO complex leads to large (ideally 180°) dihedral angle. Figure 3 shows the distributions of the dihedral angle calculated for collision energy values ranging from 1 to 77 kJ mol^{-1}. The plot was obtained by binning the dihedral angle of the reactive trajectories in boxes of 30° and normalizing the values to their maximum. As apparent from the figure, the maximum is always located at the lowest value of the dihedral angle associated with the cis-HOCO complex. At higher collision energy, a relatively large fraction (up to 34%) of breaking into products occurs via the trans–HOCO complex. However, the figure shows also that the fraction of reactive events leading to products via a breaking of the trans–HOCO complex remains at about 10% as the collision energy tends to zero. This means that this complementary reaction channel never dries up in agreement with the fact that internal energy is sufficient to feed reaction and that its partitioning between the two reactive pathways has a strong statistical character.

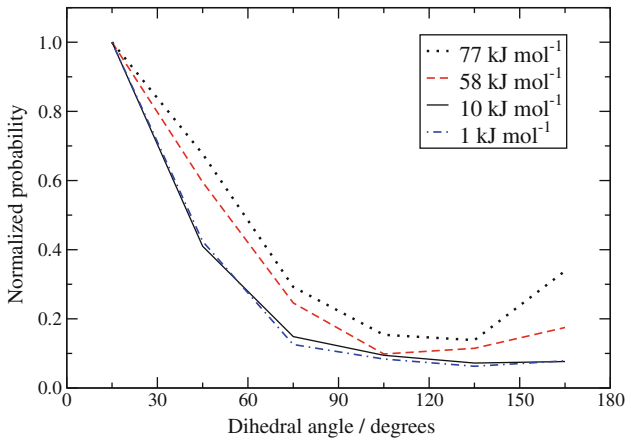

Fig. 3 Distribution of the product dihedral angle calculated on the Leiden PES for several collision energy (*lines connecting points* are shown for shake clarity). Distributions are normalized to the maximum

4 The cm product distributions

Additional information on the detailed reaction dynamics of the title system is indeed provided by the comparison of the calculated cm (the cm label will be omitted when not explicitly required to the end of avoiding misinterpretation) PTDs and PADs with the corresponding data derived by CMB studies of Refs. [19–21].

Figure 4 shows the QCT PTDs calculated on the Leiden PES (solid circles connected by dashed lines) at both experimental translational energies ($E_{tr} = 36$ (lower panel) and 59 kJ mol^{-1} (upper panel)). The distributions have been obtained using a binning method with a box of 8.4 kJ mol^{-1}. In the Figure, the distributions calculated on the YMS and LTSH PESs (dotted-dashed lines and dotted lines, respectively) as well as those obtained from the experiment (solid line) are also shown.

The PTDs calculated on the Leiden PES are largely symmetric (the average product translational energies are coincident with the value at the maxima) although the one calculated at $E_{tr} = 59$ kJ mol^{-1} is slightly broader than that calculated at $E_{tr} = 36$ kJ mol^{-1}. Both PTDs peak at a similar value, 80 and 88 kJ mol^{-1} for, respectively, $E_{tr} = 36$ and 59 kJ mol^{-1}. The two Leiden PTDs have the same shape as that obtained on the YMS PES and a shape similar to that obtained on the LTSH PES though with a maximum slightly shifted to larger translational energies (96 kJ mol^{-1} for both translational energies). However, all the PTDs calculated on the proposed PESs are definitely cooler than the experimental ones for which the measured average translational energy of the products is significantly higher than the value given by QCT calculations. This behavior is usually attributed to an insufficient repulsive nature of the proposed PESs in the exit H + CO_2 channel

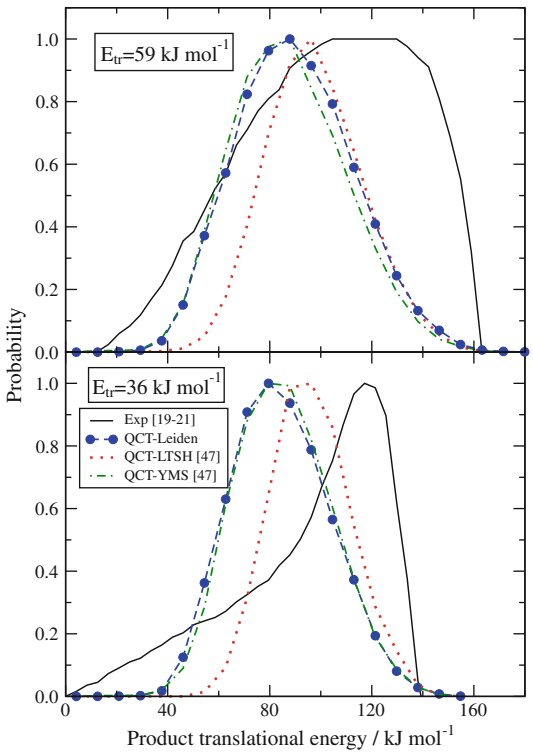

Fig. 4 QCT product translational energy distributions calculated on the Leiden PES (*solid circles* connected by *dashed lines*) at $E_{tr} = 59$ kJ mol^{-1} (*upper panel*) and 36 kJ mol^{-1} (*lower panel*). Experimental values of Refs. [19–21] are given as a *solid line* (no *error bars* are given to keep the figure simple). Results from QCT calculations on the YMS and LTSH PESs are also given as *dotted-dashed* and *dotted lines*, respectively. Distributions are normalized to the maximum

(although it could be attributed as well to an inadequate representation either of the potential energy or of the experimental conditions).

For this reason, we calculated the PTD also for $E_{tr} = 36$ kJ mol^{-1} and the initial OH radical excited at its first vibrational state. The source beam of the experiment can contain, in fact, a non-negligible fraction of vibrationally excited OH (the effect of the rotational excitation of the reactants on the shape of the calculated PTDs and PADs was not considered because it was already found in Ref. [47] to contribute negligibly). The main effect of vibrationally exciting OH, however, is to increase the amount of energy available for reaction and make the PTD extend to slightly larger product translational energy. However, no change was found in the shape of the PTD that results qualitatively similar to the one obtained for the ground vibrational state of OH. The PTD calculated on the Leiden PES for $v_{OH} = 1$ is, in fact, largely symmetric with a shift of the maximum from 80 to 88 kJ mol^{-1} that is still clearly insufficient to reproduce the shape of the experimental distribution.

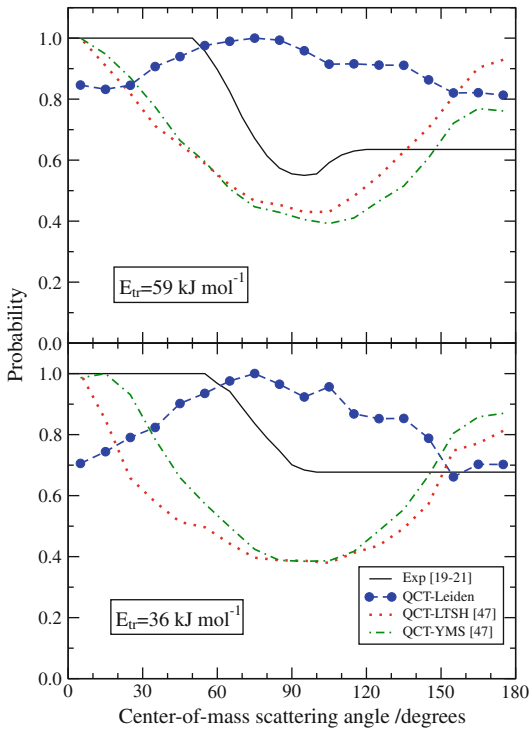

Fig. 5 QCT product angular distributions calculated on the Leiden PES (*solid circles* connected by *dashed lines*) at $E_{tr} = 59$ kJ mol^{-1} (*upper panel*) and 36 kJ mol^{-1} (*lower panel*). Experimental values of Refs. [19–21] are given as a *solid line* (no *error bars* are given to keep the figure simple). Results from QCT calculations on the YMS and LTSH PESs are also given as *dotted-dashed* and *dotted lines*, respectively. Distributions are normalized to the maximum

Figure 5 shows the QCT PADs of CO_2 (with respect to the OH initial velocity) calculated on the Leiden PES (solid circles connected by dashed lines) at both experimental translational energies $E_{tr} = 36$ (lower panel) and 59 kJ mol^{-1} (upper panel). The plotted PADs, obtained using a binning box of 10°, are largely isotropic for both collision energy values with a slightly pronounced maximum centered around 90°. This behavior is definitely anomalous with respect to those calculated on the YMS and LTSH PESs (dotted-dashed lines and dotted lines of Fig. 5, respectively) as well as with respect to those obtained from the experiment (solid line of the same figure). The lack of a forward–backward structure with a forward bias in the QCT PADs calculated on the Leiden PES cannot be ascribed to an insufficient statistics of the calculations. The number of trajectories integrated for the purpose of evaluating the product distributions at the energy of the experiment is, in fact, very large (as already mentioned, the associated statistical error is, indeed, extremely small) and largely exceeding that of any previous calculations for the title system. It cannot be ascribed to the fraction of OH excited to $v_{OH} = 1$ because the PAD calculated on the Leiden PES for it is substantially similar to that calculated for $v_{OH} = 0$. Therefore, such an anomalous PAD must be considered as a specific dynamic feature of the Leiden PES.

5 The laboratory angular distributions

The way in which the detailed comparison between theory and experiment has been carried out in the previous section is the traditional one mentioned in the Introduction: the intensity $I_{lab}(\Theta', w')$ of the scattered product measured in the CMB experiment as a function of the laboratory velocity w' and the laboratory angle Θ' is fitted by assuming that the flux in the cm framework $I_{cm}(\theta', E'_{tr})$ can be factorized in terms of $T(\theta')$ and $P(E'_{tr})$ (the PAD and the PTD, respectively). Then, a tentative PAD and PTD shape is optimized to minimize the difference between the measured data and the intensity obtained by converting the calculated flux from the cm to the lab frame. The optimized PADs and PTDs are taken as the quantities to compare with theoretical results (despite the fact that their uniqueness cannot be guaranteed).

The direct transformation in GEMS of the calculated cm quantities into the lab ones offers, instead, the possibility of generating accurate and unique calculated laboratory angular distributions (LADs) depending only on the PES adopted. Yet, due to the impossibility of deriving from the literature all the physical details of the experimental apparatus used to study the title system, we had to calculated the LAD using the less specific LAB_AD procedure of Refs. [63, 64]. In particular, we applied the mentioned procedure to the QCT output obtained at the collision energy of 59 kJ mol^{-1}. To this end, a peak velocity of the OH beam of 3,100 m s^{-1} with a speed ratio of 8.3, a peak velocity of the CO beam of 1,048 m s^{-1} with a speed ratio of 10.3 and a beam crossing angle of 90° have been used to mimic the experimental conditions [19]. The LAD resulting from the calculations performed on the Leiden PES (solid circles connected by dashed lines) is compared in Fig. 6 with that obtained from the experiment (stars connected by solid lines). In the same figure, the LAD calculated on the LTSH PES (solid squares connected by dotted lines) is also shown for further comparison. As apparent from the figure, the Leiden and the LTSH LADs show similar widths (despite the large difference in the shape of the related PADs shown in Fig. 5) differing significantly from the experimental one that is clearly broader. The LADs calculated on the Leiden and on the LTSH PESs show also two similar peaks located at about 20° and 32°–34° (clearly differing from the rather unimodal with a shoulder structure of the experimental distribution) in spite of the already pointed out differences in the calculated cm PAD. They only differ appreciably, instead, in the

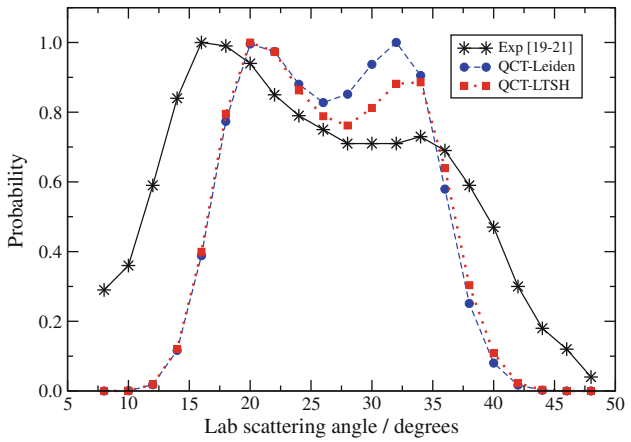

Fig. 6 QCT laboratory angular distribution calculated on the Leiden PES (*solid circles* connected by *dashed lines*) at $E_{tr} = 59$ kJ mol^{-1}. Experimental values of Refs. [19–21] are given as *stars* connected by *solid lines*. Results from QCT calculations on the LTSH PES are also given (*solid squares* connected by *dotted lines*)

amplitude of the larger Θ' peak that is lower for the LTSH results. This might indicate that the found anomaly of the PAD calculated on the Leiden PES could be smeared when considering a LAD obtained from a procedure taking in full account the experimental conditions. The effect is, however, so large to ask for further development of GEMS in the direction of incorporating exactly all the physical parameter of the experiment to be used as a tool for validating the proposed PES.

6 Conclusions

The possibility of using a full ab initio PES and a complete from first principle workflow to derive measurable properties for the $OH + CO \rightarrow H + CO_2$ reaction when utilizing the grid empowered molecular simulator GEMS has made it feasible not only to calculate the center-of-mass angular and translational distributions of products but also to derive the related LADs (laboratory angular distributions) of the corresponding CMB experiment. To this end, we have exploited two new features of GEMS explicitly developed for the present investigation and the well-established high-throughput performance of the segment of the EGEE grid available to COMPCHEM.

Thanks to that several millions trajectories have been integrated and the statistical error has been confined to a few percent at all energies (including the near threshold ones). The results of such an extended investigation are quite surprising. While the estimate of the excitation function obtained from our calculations is in line with previously published results and reconducts the contrasting indications of previous investigations to the uncertainty associated with an inadequate filtering of poorly energy conserving trajectories, the product distributions show contradictory features. In fact, the PTDs calculated on the Leiden PES agree with the ones calculated on the YMS surface, slightly differ from the LTSH ones (mainly for a shift along the energy axis) and differ even more from the experimental data. On the contrary, the PADs calculated on the Leiden PES are completely different from all the other (calculated and experimental) ones. However, when the structure of the LAD is considered, the difference between the Leiden and the LTSH results almost vanishes, while that with the experiment persists. Such an anomalous behavior could be rationalized in terms either of a particular structure of the ab initio potential energy values of the Leiden PES or of a strong differential sensitivity of the measured product intensity to the recoil angle and associated velocity distributions. This means that only a complete incorporation of the experimental parameters into the relevant section of GEMS enables a usage of the simulator as a tool for rationalizing CMB experiments. It also means, however, that the use of less sophisticated approaches is even less reliable and sometime misleading. For this reason, our next effort will be a detailed scrutiny of the used PES and a complete implementation of the theoretical assemblage of the LAD.

Acknowledgments The Leiden ab initio results were kindly supplied to us by R. Valero and G.J. Kroes. The LAB_AD program was kindly supplied to us by F.J. Aoiz. Partial financial support from Spanish MICINN (CTQ-2008-02578/BQU), Italian MIUR, EGEE-III and ARPA Umbria is acknowledged. This work has been carried out also as part of the activities of the cooperation scheme of the QDYN working group of the COST CMST European Cooperative Project CHEMGRID (Action D37). Computational assistance and resources were provided by the IZO-SGI SGIker (UPV/EHU, MICINN, GV/EJ, ESF), Spanish Supercomputing Network (BSC-RES) and CINECA.

References

1. Warnatz J, Maas U, Dibble RW (2006) Combustion: physical and chemical fundamentals, modeling and simulation, experiments, pollutant formation, 4th edn. Springer, Berlin
2. Miller JA, Kee RJ, Westbrook CK (1990) Annu Rev Phys Chem 41:345
3. Wayne RP (2000) Chemistry of atmospheres. Oxford University Press, Oxford
4. Finlayson-Pitts BJ, Pitts JN (2000) Chemistry of the upper and lower atmosphere theory. Academic Press, London
5. Westenberg AA, deHaas NJ (1973) J Chem Phys 58:4061
6. Vandooren J, Peters J, Van Tiggelen PJ (1975) Proc Combust Inst 15:745
7. Ravishankara AR, Thompson RL (1983) Chem Phys Lett 99:377
8. Wooldridge MS, Hanson RK, Bowman CT (1994) Proc Combust Inst 25:741
9. Lissianski V, Yang H, Qin Z, Mueller MR, Shin KS, Gardiner WC Jr (1995) Chem Phys Lett 240:57
10. Wooldridge MS, Hanson RK, Bowman CT (1996) Int J Chem Kinet 28:361

11. Feilberg KL, Sellevåg SR, Nielsen CJ, Griffith WDT, Johnson MS (2002) Phys Chem Chem Phys 4:4687
12. Fulle D, Hamann HF, Hippler H, Troe J (1996) J Chem Phys 105:983
13. Golden DM, Smith GP, McEwen AB, Yu CL, Eiteneer B, Frenklach M, Vaghjiani GL, Ravishankara AR, Tully FP (1998) J Phys Chem A 102:8598
14. Senosiain JP, Musgrave CB, Golden DM (2003) Int J Chem Kinet 35:464
15. Senosiain JP, Klipenstein SJ, Miller JA (2005) Proc Combust Inst 30:945
16. Li J, Zhao Z, Kazakov A, Chaos M, Dryer FL, Scire JJ Jr (2007) Int J Chem Kinet 39:109
17. Wolfrum J (1987) Faraday Discuss Chem Soc 84:191
18. Koppe S, Laurent T, Volpp HR, Wolfrum J, Naik PD (1996) In: 26th symposium (Int) on combustion, The Combustion Institute, Pittsburgh, 489
19. Alagia M, Balucani N, Casavecchia P, Stranges D, Volpi GG (1993) J Chem Phys 98:8341
20. Alagia M, Balucani N, Casavecchia P, Stranges D, Volpi GG (1995) J Chem Soc Faraday Trans 91:575
21. Casavecchia P, Balucani N, Volpi GG (1995) In: Liu K, Wagner A (eds) The chemical dynamics and kinetics of small radicals. World Scientific, Singapore
22. Zhu RS, Diau EGW, Lin MC, Mebel AM (2001) J Phys Chem A 105:11249
23. Chen WC, Marcus RA (1995) J Chem Phys 123:094307
24. Chen WC, Marcus RA (1995) J Chem Phys 124:024306
25. Joshi AV, Wang H (2006) Int J Chem Kinet 38:57
26. Bowman JM, Schatz GC (1995) Annu Rev Phys Chem 46:169
27. Kudla K, Schatz GC (2005) In: Liu K, Wagner A (eds) The chemical dynamics and kinetics of small radicals. World Scientific, Singapore
28. Clary DC, Schatz GC (1993) J Chem Phys 99:4578
29. Hernández MI, Clary DC (1994) J Chem Phys 101:2779
30. Goldfield EM, Gray SK, Schatz GC (1995) J Chem Phys 102:8807
31. Zhang DH, Zhang JZH (1995) J Chem Phys 103:6512
32. Balakrishnan N, Billing GD (1996) J Chem Phys 104:4005
33. Dzegilenko FN, Bowman JM (1998) J Chem Phys 108:511
34. Billing GD, Muckerman JT, Yu HG (2002) J Chem Phys 117:4755
35. Valero R, Kroes GJ (2002) J Chem Phys 117:8736
36. McCormack DA, Kroes GJ (2003) Chem Phys Lett 352:281; Erratum, ibid. 373:648
37. Lakin MJ, Troya D, Schatz GC, Harding LB (2003) J Chem Phys 119:5848
38. Medvedev DM, Gray SK, Goldfield EM, Lakin MJ, Troya D, Schatz GC (2004) J Chem Phys 120:1231
39. He Y, Goldfield EM, Gray SK (2004) J Chem Phys 121:823
40. Valero R, McCormack DA, Kroes GJ (2004) J Chem Phys 120:4263
41. Valero R, van Hemert MC, Kroes GJ (2004) Chem Phys Lett 393:236
42. Valero R, Kroes GJ (2004) Phys Rev A 70:040701
43. Valero R, Kroes GJ (2004) J Phys Chem A 108:8672
44. Valero R, Kroes GJ (2006) Chem Phys Lett 417:43
45. Zhang S, Medvedev DM, Goldfield EM, Gray SK (2006) J Chem Phys 125:164312
46. Song X, Li J, Hou H, Wang B (2006) J Chem Phys 125:094301
47. Garcia E, Saracibar A, Zuazo L, Laganà A (2007) Chem Phys 332:162
48. Sun HY, Law CK (2008) J Mol Struc 862:138
49. Schatz GC, Fitzcharles MS, Harding LB (1987) Faraday Discuss Chem Soc 84:359
50. Yu HG, Muckerman JT, Sears TJ (2001) Chem Phys Lett 349:547
51. Murrell JN, Carter S, Farantos SC, Huxley P, Varandas AJC (1984) Molecular potential energy functions. Wiley, Chichester
52. Yang M, Zhang DH, Collins MA, Lee SY (2001) J Chem Phys 115:174
53. Gervasi O, Laganà A, Costantini A (2004) Future Gener Comput Syst 20:703
54. Gervasi O, Crocchianti S, Pacifici L, Skouteris D, Laganà A (2006) Lect Ser Comput Comput Sci 7:1425
55. Gervasi O, Manuali C, Laganà A, Costantini A (2009) ICTP Lect Notes 84:63
56. Rampino S, Monari A, Evangelisti S, Rossi E, Rud K, Laganà A (2010) In: Bubak M, Turala M, Wiatr K (eds) Proceedings of the Cracow'09 grid workshop, ACC CYFRONET AGH, Cracow (ISBN 9788361433019)
57. Hase WL, Duchovic RJ, Hu X, Komornicki A, Lim KF, Lu D, Peslherbe GH, Swamy KN, Van de Linde SR, Varandas AJC, Wang H, Wolf RJ (1996) QCPE Bull 16:43
58. EGEE: Enabling Grids for E-Sciene in Europe. http://www.eu-egee.or. Accessed 1 March 2010
59. Barcelona Supercomputing Centre. http://www.bsc.e. Accessed 1 March 2010
60. CINECA: Supercomputing Centre, Consortium of Universities. http://www.cineca.i. Accessed 1 March 2010
61. Laganà A, Riganelli A, Gervasi O (2006) Lect Notes Comput Sci 3980:665
62. Troya D, Lakin MJ, Schatz GC, González M (2001) J Chem Phys 115:1828
63. Aoiz FJ, Bañares L, Herrero VJ, Saéz-Rábanos V, Stark K, Werner HJ (1995) J Chem Phys 102:9248
64. Aoiz FJ, Verdasco E, Saéz-Rábanos V, Loech HJ, Menéndez M, Stienkemeier F (2000) Phys Chem Chem Phys 2:541